Supplementary information for

Physicochemical aspects of mucosa surface

Mary Avgidou[a], Maria Dimopoulou[ab], Alan R. Mackie[c], Neil M. Rigby[c], Christos Ritzoulis[bd], Constantinos Panayiotou[*a]

CONTENTS

[a]*Department of Chemical Engineering, Aristotle University of Thessaloniki, 54024 Thessaloniki, Greece*

[b]*Department of Food Technology, ATEI Thessaloniki, 57400 Thessaloniki, Greece*

[c]*Institute of Food Research, Norwich Research Park, Colney Lane, Norwich Research Park, Norwich NR4 7UA, U.K*

[d]*School of Food Science and Bioengineering, Zhejiang Gongshang University, Xiasha, Hangzhou, Zhejiang 310016, China*

*Corresponding author: E-mail: cpanayio@auth.gr; Fax: +30 2310-996223; Tel: +30 2310-996223

S.1. Physico-chemical characterization

TMDSC analysis. Temperature-modulated differential scanning calorimetry (TMDSC) analysis of the mucin of the column material was performed in the temperature range between -20 and +230°C. From the recorded scan shown in Fig. S.1a, it is observed that the variation of the total heat flow follows that of the nonreversing across the whole temperature range of scanning. Two endothermic regions are apparent at about 0 and over 140°C, with the first attributed to a start-up hook due to differences in the heat capacity between the sample and the reference pans at the very beginning (2–3 min) of the scan[1], and the second being a stepwise endothermic region due to decomposition changes of the polymer. Processing of the second-order transition observed between 40 and 120°C in the magnification of the reversing heat flow of Fig. S.1b, resulted in a T_g value equal to 82.5°C. Available literature DSC data for pig mucin concern gastric mucosa[2] and report a glass transition at a somewhat lower temperature range (onset 40.4°C, end 68.6°C), probably due to differences in the sample origin and/or conditioning.

TGA analysis. Thermo-gravimetric analysis (TGA) of the mucin of the column material shows two mass loss steps (Fig. S.2). The first ends at about 100°C, and results in a mass loss of 4%, possibly due to the removal of the remaining humidity. The next step, detected above 140°C, is attributed to the decomposition onset, and it is in accordance with the above DSC results.

XRD analysis. Fig. S.3 presents the X-ray (XRD) angular diffraction intensity plot of the as received mucin material. It appears to form an amorphous body, as indicated by a broad peak roughly spanning 2θ values from 12° to 43°.

FTIR analysis. The infra red (FTIR) spectrum of the mucin of the column material is shown in Fig. S.4. The so-called fingerprint region of the spectrum consists of characteristic peaks centered at 1637 and 1537 cm^{-1}, which are attributed to the amide I and amide II region, respectively[3,4], of the amino acids contained in the macromolecular backbone. In addition, the characteristic peaks between 1400 and 1000 cm^{-1} can be attributed to the glycans that cover the protein backbone.[5] The sharp band at 2919 cm^{-1} is characteristic of C–H stretching[6], while the broader band centered at 3274 cm^{-1} is due to the hydrogen-bonding between hydroxyl groups.[7] Of interest to the above is the extent of the hydrogen bonding observed as a very wide peak.
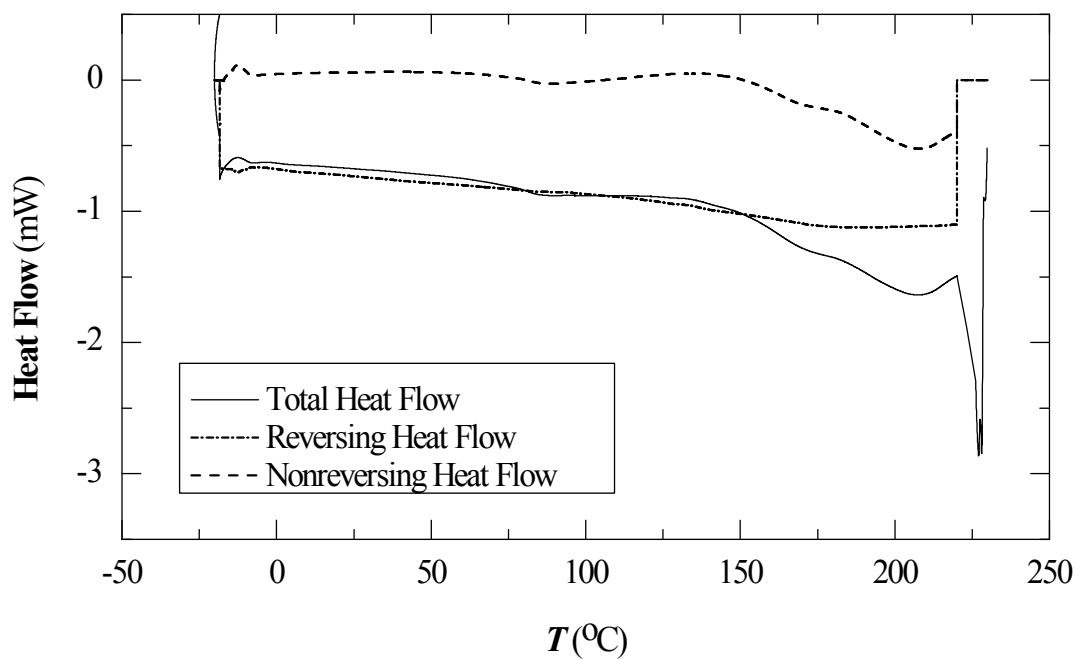
a)
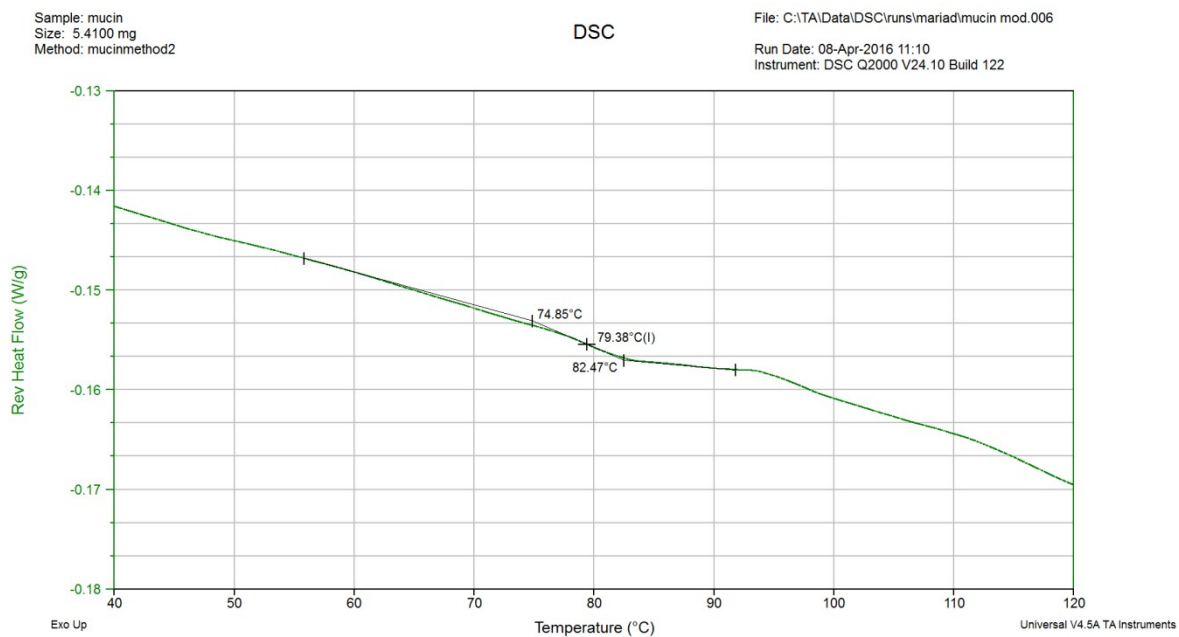
b)

Fig. S.1 a) TMDSC thermograms of the examined porcine mucin sample (heating rate: 5°C min^{-1}; temperature modulation: 1°C amplitude, 60 s period), and b) processing of the second-order sigmoidal shift in the baseline of the reversing heat flow.
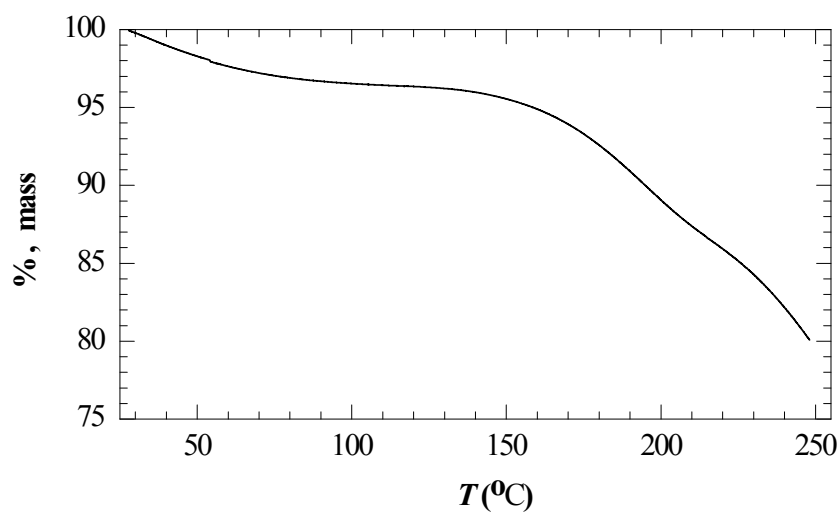
Fig. S.2 Thermogravimetric (TGA) analysis of the examined porcine mucin sample (heating rate 5°C/min).
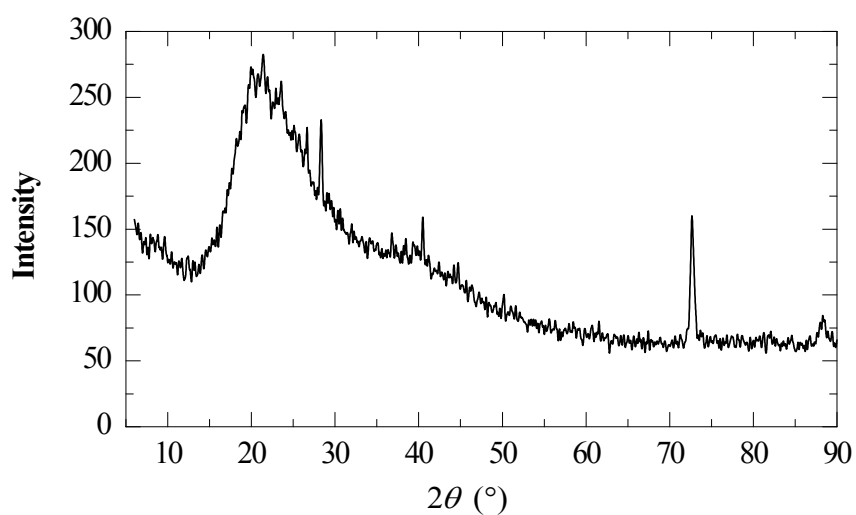

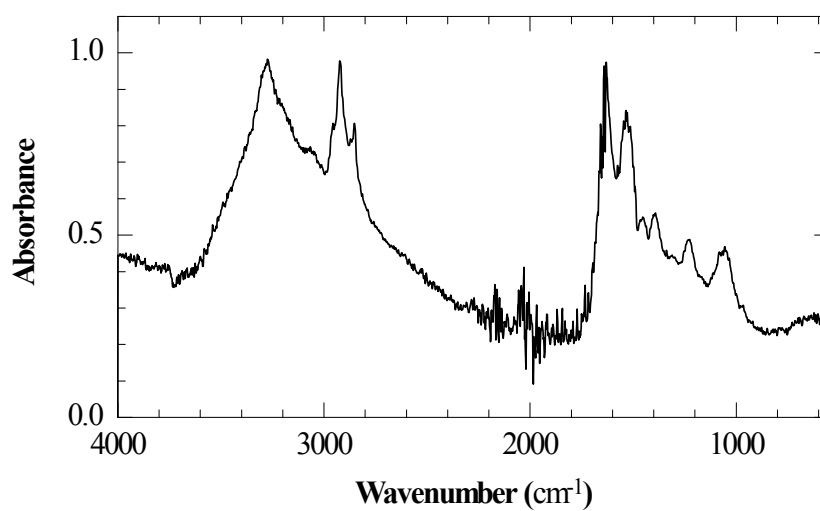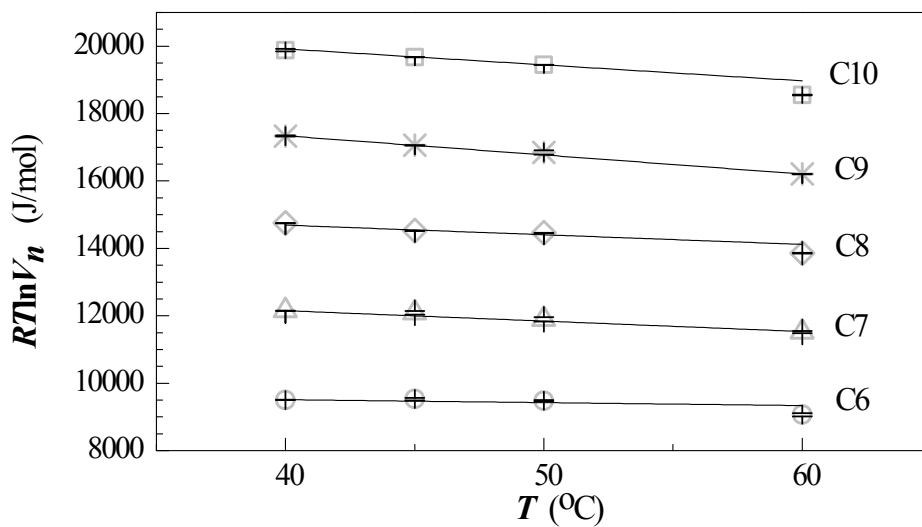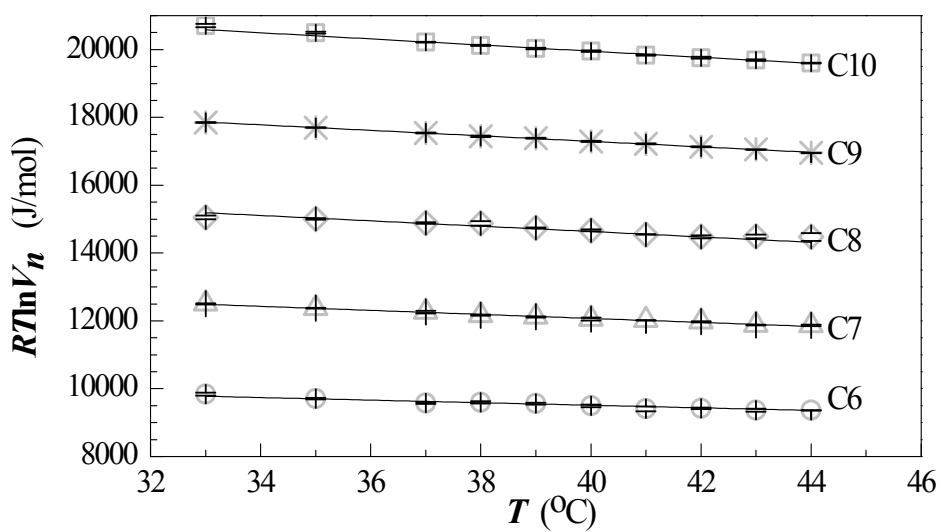**Fig. S.3** X-ray diffractogram of the as received mucin material.

Fig. S.4 Fourier transform IR spectra of the examined porcine mucin sample.

S.2.   Supplementary data of IGC study

a)

b)

Fig. S.5 Variation of $RT\ln V_n$ data of n-alkanes with temperature at a) 40–60°C, and b) 33–44°C. The linear form is typical for physical sorption, while the minute confidence intervals (depicted inside the symbols of the graphs) confirm the high reproducibility of the retention volume measurements.

Table S.1 Physicochemical properties of the tested probes

Probe	T_b (°C)	M (kg kmol^{-1})	n	V_m (ml/mol)				AN* (kJ mol^{-1})	DN (kJ mol^{-1})	Character
				40°C	45°C	50°C	60°C			
Hexane	68.7	86.2	1.373	134.17	135.15	136.16	138.27	n/a	n/a	neutral
Heptane	98.4	100.2	1.386	149.85	150.84	151.85	153.93	n/a	n/a	neutral
Octane	125.7	114.2	1.394	166.22	167.21	168.22	170.30	n/a	n/a	neutral
Nonane	150.8	128.3	1.406	182.47	183.47	184.49	186.60	n/a	n/a	neutral
Decane	174.1	142.3	1.409	198.88	199.94	201.01	203.21	n/a	n/a	neutral
Methyl acetate	56.9	74.1	1.361	81.56	82.18	82.80	84.11	6.7	69.1	amphoteric
Ethyl acetate	77.1	88.1	1.372	100.62	101.32	102.05	103.55	6.3	71.6	amphoteric
THF	66	72.1	1.405	83.48	84.01	84.56	85.69	2.1	83.7	basic
Chloroform	62	119.4	1.446	82.06	82.60	83.16	84.31	22.6	0	acidic
Pyridine	115.2	79.1	1.510	82.18	82.62	83.08	84.01	0.6	138.6	basic
Acetonitrile	81.6	41.1	1.344	53.98	54.38	54.78	55.61	19.7	59.0	amphoteric
n-Butanol	118	74.1	1.399	93.43	93.93	94.44	95.50	38.1	0	acidic
Ethanol	78.4	46.1	1.361	59.65	60.01	60.39	61.16	43.1	79.6	amphoteric

M, n values were cited from Ref. 8; T_b values were cited from Ref. 9,10; V_m values were calculated from parametric formulas cited from Ref. 9,10; AN*, DN values were cited from Ref. 11.

Table S.2 Coefficients of the linear regression of $RT\ln V_n$ of n-alkanes versus the carbon number estimated in: a) the 1st experimental series (Fig. 3a), and b) the 2nd experimental series (Fig. 3b)

a)

T (°C)	ΔG^{CH_2} (slope)	intercept	R^2
40	2594.5 ± 10.6	-6031.9 ± 85.9	0.9999
45	2525.7 ± 17.0	-5630.6 ± 138.1	0.9998
50	2488.5 ± 19.0	-5484.7 ± 154.1	0.9998
60	2366.4 ± 12.3	-5092.8 ± 100.0	0.9999

b)

T (°C)	ΔG^{CH_2} (slope)	intercept	R^2
33	2707.8 ± 35.2	-6475.6 ± 285.9	0.9995
35	2687.8 ± 21.3	-6453.2 ± 172.7	0.9998
37	2653.9 ± 6.1	-6338.4 ± 50.0	1
38	2631.8 ± 13.2	-6216.6 ± 107.1	0.9999
39	2619.7 ± 10.7	-6192.6 ± 86.7	0.9999
40	2613.1 ± 12.9	-6218.8 ± 104.6	0.9999
41	2605.5 ± 11.7	-6238.4 ± 94.7	0.9999
42	2582.0 ± 17.1	-6106.2 ± 139.1	0.9998
43	2582.4 ± 11.3	-6162.6 ± 91.8	0.9999
44	2557.7 ± 15.3	-6010.6 ± 124.5	0.9999

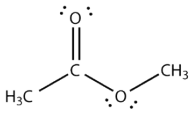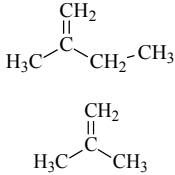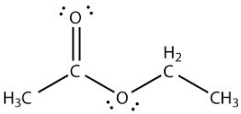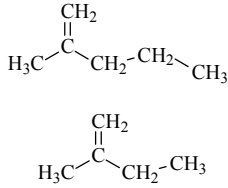**Table S.3** Correspondence of polar probes to hydrocarbon homomorphs
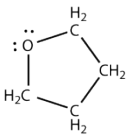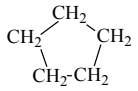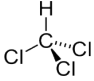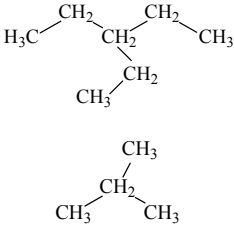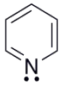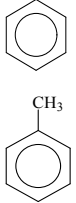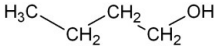
Polar probe	Corresponding Homomorph

Methyl acetate

2-Methyl-1-butene

correction: Isobutene

Ethyl acetate

2-Methyl-1-pentene

correction: 2-Methyl-1-butene

THF

Cyclo-pentane

Chloroform
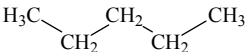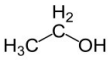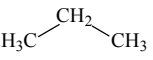
3-Ethyl-pentane

correction: Isobutane

Pyridine

Benzene

correction: Toluene

Acetonitrile

$H_3C-C\equiv N$

Propyne (Methylacetylene)

$H_3C-C\equiv CH$

n-Butanol

n-Pentane

Ethanol

Propane

Table S.4 Physical properties of the corresponding, to polar probes, hydrocarbon homomorphs

Polar probe	Corresponding Homomorph	T_b (°C)	M (kg kmol^{-1})	V_m (ml mol^{-1})			
				40°C	45°C	50°C	60°C
Methyl acetate	2-Methyl-1-butene	31.2	70.1	111.57	112.58	113.63	115.83
	correction: Isobutene	-6.9	56.1	98.66	99.85	101.11	103.82
Ethyl acetate	2-Methyl-1-pentene	62.1	84.2	127.48	128.44	129.43	131.50
	correction: 2-Methyl-1-butene	31.2	70.1	111.57	112.58	113.63	115.83
THF	Cyclo-pentane	49.3	70.1	96.33	96.93	97.55	98.84
Chloroform	3-Ethyl-pentane	93.5	100.2	146.94	147.92	148.93	151.01
	correction: Isobutane	-11.7	58.1	109.05	110.46	111.94	115.16
Pyridine	Benzene	80.1	78.1	91.07	91.62	92.18	93.34
	correction: Toluene	110.6	92.1	108.31	108.91	109.52	110.78
Acetonitrile	Propyne (Methylacetylene)	-23.2	40.1	68.63	69.59	70.61	72.85
n-Butanol	*n*-Pentane	36.1	72.1	118.99	120.03	121.11	123.38
Ethanol	Propane	-42	44.1	94.71	96.61	98.70	103.56

M, n values were cited from Ref. 8; T_b values were cited from Ref. 9,10; V_m values were calculated from parametric formulas cited from Ref. 9,10.

References of supplementary information

1   L.C. Thomas, Thermal Analysis Review: Interpreting Unexpected Events and Transitions in DSC Results, *Thermal Analysis Technical Publications*, TA Instruments, Inc., 1996.

2   P.F. Builders, O.O. Kunle and M.U. Adikwub, *Int. J. Pharm*., 2008, **356**, 174–180.

3   P.F. Builders, N. Ibekwe, L.C. Okpako, A.A. Attama and O.O. Kunle, *Eur. J. Pharm. Biopharm.*, 2009, **72**, 34–41.

4   E.J. Castillo, J.L. Koenig, J.M. Anderson and N. Jentoft, *Biomaterials*, 1986, **7**, 9–16.

5   M. Kacuráková and R.H. Wilson, *Carbohydr. Polym.*, 2001, **44**, 291–303.

6   C.A. Silva, T.M. Nobre, F.J. Pavinatto and O.N. Oliveira Jr., *J. Colloid Interface Sci.*, 2012, **376**, 289–295.

7   J. Kong and S. Yu, *Acta Biochim Biophys Sinica*, 2007, **39**, 549–559.

8   "Physical Constants of Organic Compounds", Section 3 in *CRC Handbook of Chemistry and Physics*, Internet Version 2005, Lide D.R., ed., http://www.hbcpnetbase.com (accessed October 2015).

9   T. E. Daubert and R. P. Danner, Data Compilation Tables of Properties of Pure Compounds, *AIChE Symp Ser. No. 203*, American Institute of Chemical Engineers, New York, 1985.

10 T.E. Daubert and R.P. Danner, *Physical and Thermodynamic Properties of Pure Compounds: Data Compilation*, Hemisphere, New York, 2001.

11 A. van Asten, N. van Veenendaal and S. Koster, *J. Chromatogr. A*, 2000, **888**, 175–196.